ORIGINAL ARTICLE

Pulmonary function, CT and echocardiographic abnormalities in sickle cell disease

Alan Lunt,[1,2] Sujal R Desai,[3] Athol U Wells,[4] David M Hansell,[4] Sitali Mushemi,[3] Narbeh Melikian,[3] Ajay M Shah,[2,5] Swee Lay Thein,[2,6] Anne Greenough[1,2]

[1]Division of Asthma, Allergy and Lung Biology, MCR Centre for Allergic Mechanisms in Asthma, King's College London, London, UK
[2]National Institute for Health Research (NIHR) Biomedical Research Centre based at Guy's and St Thomas' NHS Foundation Trust and King's College London, London, UK
[3]Department of Radiology and Interstitial Lung Unit, King's College London, London, UK
[4]Department of Radiology, Royal Brompton Hospital, London, UK
[5]Cardiovascular Division, King's College London British Heart Foundation Centre, London, UK
[6]Division of Cancer Studies, King's College London and Dept Haematological Medicine, King's College Hospital, London, UK

Correspondence to
Professor Anne Greenough, Neonatal Intensive Care Centre, 4th Floor Golden Jubilee Wing, King's College Hospital, Denmark Hill, London SE5 9RS, UK; anne.greenough@kcl.ac.uk

ABSTRACT

Objectives To test the hypothesis that vascular abnormalities on high-resolution CT (HRCT) would be associated with echocardiographic changes and lung function abnormalities in patients with sickle cell disease (SCD) and the decline in lung function seen in SCD patients.

Methods HRCT, echocardiography and lung function assessments were made in 35 adults, 20 of whom had previously been assessed a median of 6.6 years prior to this study. The pulmonary arterial dimensions on HRCT were quantified as the mean segmental pulmonary artery/bronchus (A/B) ratio and the summated cross-sectional area of all pulmonary vessels <5 mm in diameter (cross-sectional area (CSA)<5 mm%).

Results The segmental A/B ratio was negatively correlated with FEV_1, vital capacity (VC), forced expiratory flow between 25% and 75% of VC ($FEF_{25/75}$) and arterial oxygen saturation (SpO_2) and positively with the residual volume: total lung capacity ratio (RV:TLC) and respiratory system resistance (Rrs). CSA<5 mm% was negatively correlated with FEV_1, $FEF_{25/75}$ and SpO_2 and positively with RV, RV:TLC and respiratory system resistance (Rrs). There were significant correlations between cardiac output assessed by echocardiography and the segmental A/B ratio and CSA<5 mm%. Lung function (FEV_1 p=0.0004, VC p=0.0347, $FEF_{25/75}$ p=0.0033) and the segmental A/B ratio (p=0.0347) and CSA<5 mm% (p<0.0001) significantly deteriorated over the follow-up period.

Conclusions Abnormalities in pulmonary vascular volumes may explain some of the lung function abnormalities and the decline in lung function seen in adults with SCD.

INTRODUCTION

Sickle cell disease (SCD) is one of the commonest inherited disorders worldwide, affecting an estimated 300 000 newborns every year.[1] With improved general healthcare, the majority of patients with SCD in developed countries can expect to survive to adulthood. In adulthood, however, SCD can be associated with multiorgan damage, including pulmonary complications. Acute chest syndrome is the commonest cause of death in young adults, and pulmonary dysfunction is a major contributor to morbidity in aging adults with SCD. Lung function abnormalities are common in adults with SCD.[2–7] Adults with SCD can suffer from parenchymal lung disease and pulmonary vascular disease or both; affected individuals can suffer premature death. Echocardiographic

Key messages

What is the key question?
► Vascular abnormalities on high-resolution CT (HRCT) would be associated with echocardiographic changes and lung function abnormalities in patients with sickle cell disease (SCD) and with the decline in lung function seen in SCD patients.

What is the bottom line?
► We have demonstrated an association between small vessel pulmonary vascular dimensions on HRCT reflecting pulmonary vascular volume, lung function abnormalities and echocardiographic estimates of ventricular function and cardiac output in adults with SCD; in addition, the decline in lung function correlated with changes in vascular dimension.

Why read on?
► Alterations in pulmonary vascular volumes due to anaemia in SCD patients may be responsible for some of their lung function abnormalities and changes seen on HRCT and their decline in lung function.

abnormalities consistent with raised pulmonary artery systolic pressure (PAP) suggestive of pulmonary hypertension occur in approximately 30% of adult SCD patients [8–10] and are associated with increased morbidity and mortality.[8 9 11] Right heart catheterisation studies, however, have demonstrated that only a proportion of SCD patients have pulmonary arterial hypertension (PH), that is, elevated pulmonary arterial vascular resistance, and it is the presence of PH that is associated with early death.[12] Nevertheless, elevated tricuspid valve regurgitant velocities demonstrated by echocardiography and thought to be suggestive of raised PAP are independently predictive of mortality.[8 13]

We have previously demonstrated that the majority of a cohort of adult patients with SCD had pulmonary abnormalities on high-resolution CT (HRCT).[7] The HRCT findings significantly correlated with pulmonary function testing results; in particular, there were correlations between reductions in FVC and FEV_1 and the prominence of the central vessels on HRCT. Prominent central vessels were found on HRCT in eight of the nine patients
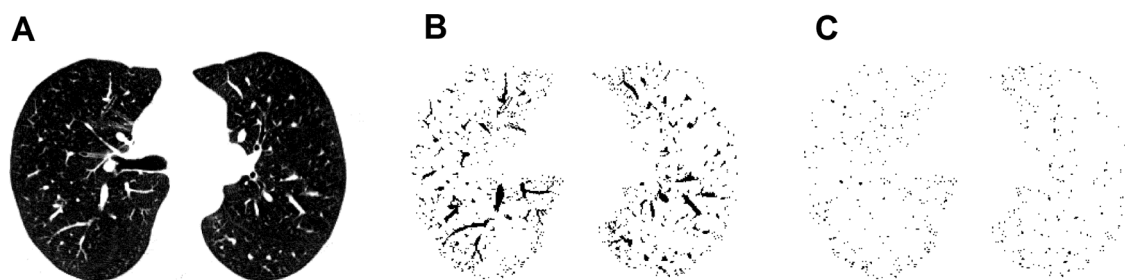
Figure 1 Measurement of cross-sectional area (CSA)<5 mm% using ImageJ software. (A) High-resolution CT image of lung field segmented with threshold values of −500 to −1024 HU. (B) Segmented image converted to binary image with window level of −720 HU, with pulmonary vessels displayed in black. (C) Mask image for particle analysis with vessel size set to 0–5 mm^2 and the circularity from 0.9 to 1.0.

with restrictive abnormalities. The prominent central vessels may reflect the raised pulmonary capillary blood volume as a result of chronic anaemia causing an increased cardiac output (CO)[14] and dilation of the pulmonary vessels.[15] We have demonstrated in SCD children that the increased pulmonary capillary blood volume contributes to their increased airways obstruction.[16] Hence, we hypothesised that the central vessel prominence would be associated with echocardiographic changes and lung function abnormalities. The aim of this study was to test that hypothesis by prospectively undertaking HRCT studies, lung function and echocardiographic assessments. A further aim of this study was to reassess the cohort examined 7 years ago[7] to determine whether any decline in lung function correlated with vascular changes evidenced by HRCT studies.

METHODS
Adults with SCD were assessed between 2009 and 2013. Subjects included in the previous study[7] had initially been assessed between 2003 and 2005. All participants gave written informed consent.

Lung function assessments
FEV_1, vital capacity (VC), forced expiratory flow between 25 and 75% of VC ($FEF_{25/27}$), total lung capacity (TLC), residual volume (RV) and mean respiratory system resistance (Rrs) were measured.

CT
CT patterns were quantified independently by two thoracic radiologists blinded to the clinical and functional data. The extent and severity of CT abnormalities were recorded in individual lobes, the lingula being considered a separate lobe for scoring purposes. Distal vessel dimensions, including both arteries and veins at the sub-subsegmental level,[17] were measured using the method of Matsuoka et al.[18 19] The total summated cross-sectional area for the vessels was then expressed as a percentage of the total lung area of the three selected slices using threshold values between −500 and −1024 HU (cross-sectional area (CSA)<5 mm%) (figure 1). The mean segmental artery/bronchus (A/B) ratio in at least three of four lobes was calculated. CT total lung volume (TLV$_{CT}$) was derived using a proprietary lung segmentation algorithm (figure 2). For the longitudinal analyses, initial and follow-up CT scans were compared.

Echocardiography
Two-dimensional and three-dimensional transthoracic echocardiography was performed according to the international guidelines.[20] Examinations were performed using digital acquisitions on a Phillips Sonos 7500 ultrasound system. Valvular

regurgitation was graded from Doppler determinations of transvalvar flow. Tricuspid regurgitation (TR) was assessed in the parasternal right ventricular inflow, parasternal short axis and apical four-chamber views. A minimum of five sequential complexes were recorded. Continuous-wave Doppler signals of the peak regurgitant jet velocities (TRV) (normal <2.5 m/s) were used to estimate the right ventricular systolic pressures (RVSP) using the Bernoulli equation (ie, 4 × [tricuspid regurgitant jet velocity]^2). PAP (normal <25 mm Hg) was calculated as the sum of RVSP and right atrial systolic pressures. CO (normal range 4.0–8.0 L/s) and right-ventricular diastolic volumes (RVDV) (normal range 100–160 mL) were also measured. Right and left ventricular function were assessed by measurement of the tricuspid annular plane systolic excursion (TAPSE) (normal >1.5 cm) and the ratio of early diastolic LV inflow (E) to lateral mitral annulus velocity (e′) measured by tissue Doppler (E/e′) (normal <8). Technically acceptable TAPSE measurements were available in 32 patients and E/e′ in 33 patients.

Statistical analysis
See online supplement.

RESULTS
Subjects
Thirty-five patients with a median age of 43 (range 17–73) years were assessed. In total, 20 of the 35 patients (median age at
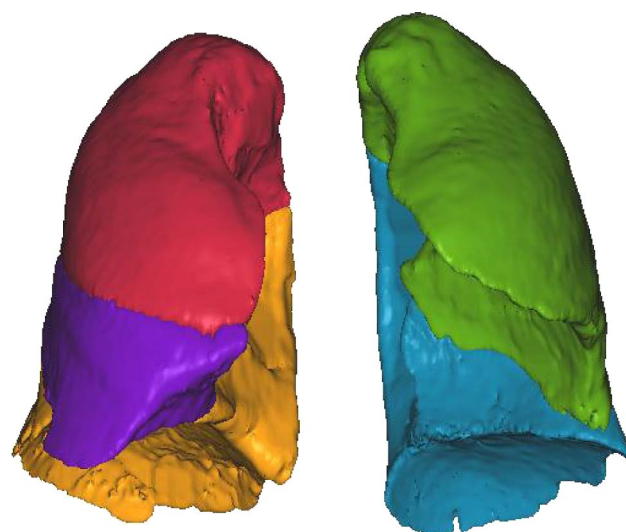

Figure 2 Example of a segmented CT examination used to derive CT total lung volume (TLV$_{CT}$). The lobes are shown in different colours.

Table 1 Lung function test results

	Median (range)
FEV_1	77.4 (27.4–114.2)
VC	81.3 (27.8–113.0)
FEV_1:VC	96.3 (75.9–115.8)
$FEF_{25/75}$	69.6 (13.7–129.2)
TLC	87.8 (63.8–109.6)
RV	93.5 (50.1–162.6)
RV:TLC	106.3 (64.6–197.4)
DLCOc	73.6 (43.9–104.8)
KCOc	94.0 (67.5–124.8)
Rrs(0)	128.2 (79.4–209.0)
Rrs(1) (kPa L^{-1} s^{-1} Hz)*	0.018 (0.001–0.042)
SpO_2 (%)*	96.0 (85.0–100.0)

*Data are presented as per cent predicted for height, age and sex except where indicated.
RV:TLC, residual volume:total lung capacity ratio; VC, vital capacity.

initial assessment 38, range 17–66 years) had been assessed at a median of 6.6 (range 5.5–6.7) years previously.

Lung function test results

There was a wide variation in the lung function of the cohort (table 1). In total, 28 of the 35 patients (80%) had lung function abnormalities: 8 (23%) had a restrictive abnormality, 6 (17%) an obstructive abnormality, 4 (11%) a mixed abnormality and 10 (29%) an isolated reduction in carbon monoxide diffusing capacity (DLCO). Six patients (17%) had a significant response to bronchodilator; three had an obstructive, one a mixed and one a restrictive abnormality, and one no lung function abnormality. Sixteen patients (46%) had elevated Rrs; six of whom otherwise had normal lung function.

HRCT abnormalities

A reticular pattern on HRCT was the most prevalent and extensive abnormality, seen in 26 patients (median 5 (range 0–17.5) %). Ground glass opacification was present in nine patients (median extent 0 (range 0–3)). Consolidation was seen in nine patients (median extent 0.4 (0–4.2)). Reduction in lobar volume was seen in 19 patients (median severity 1 (range 0–7)). Linear bands were seen in 23 patients (median 1 (range 0–6)) and subpleural curvilinear lines in 9 patients (median 0 (range 0–3)).

Subpleural consolidation (n=6), thickened interlobular septa (n=2), infarcts (n=7) and traction bronchiectasis (n=0) were present in a minority of patients and excluded from further analysis. The median pulmonary artery to ascending aorta ratio (PA/AA) was 0.90 (range 0.8–1.30), the A/B ratio 1.30 (range 1.0–2.50) and CSA<5 mm% 0.48 (range 0.22–10.2). The extent of a reticular pattern was positively correlated with the presence of linear bands (r=0.64, p<0.0001) and ground glass opacification score (r=0.42, p=0.0115). The presence of linear bands was positively correlated with subpleural curvilinear lines (r=0.39, p=0.0204), which were positively related to the A/B ratio (r=046, p=0.0056). The A/B ratio and CSA<5 mm% were positively correlated (r=0.72, p<0.0001).

Relationships between pulmonary function and HRCT results

Subpleural curvilinear lines were negatively correlated with FEV_1 (r=−0.39, p=0.0230) and $FEF_{25/75}$ (r=−0.44, p=0.0403), and the extent of a reticular pattern was negatively correlated with Rrs(0) (r=−0.40, p=0.0198). TLV_{CT} was positively correlated with FEV_1 (r=0.57, p=0.0014), VC (r=0.66, p < 0.0001) and TLC (r=0.82, p<0.0001). The segmental A/B ratio was negatively correlated with FEV_1 (r=−0.53, p=0.0011), VC (r=−0.48, p=0.0036), $FEF_{25/75}$ (r=−0.44, p=0.0403) and SpO_2 (r=−0.47, 0.0037), and positively with RV:TLC (r=0.45, p=0.0073), and Rrs(1) (r=0.22, p=0.0267). The CSA<5 mm% was negatively correlated with FEV_1 (r= −0.71, p<0.0001), VC (r=−0.72, p<0.0001), $FEF_{25/75}$ (r= −0.51, p=0.0010) and SpO_2 (r=−0.44, p=0.0070), and positively to RV (r=0.51, p=0.0020), RV:TLC (r=0.695, p<0.0001), Rrs(0) (r=0.35, p=0.0417) and Rrs(1) (r=0.67, p<0.0001).

The segmental A/B ratio and CSA<5 mm% exhibited a strong degree of multicollinearity. Therefore, separate models were generated with segmental A/B ratio or CSA<5 mm% as predictors. On stepwise regression, the segmental A/B ratio was independently related to a reduced FEV_1, VC, $FEF_{25/75}$ and SpO_2 and to an increased RV, RV:TLC, Rrs(0) and Rrs(1) (table 2). Linear bands were independently linked to a reduced FVC and TLC (table 2). The CSA<5 mm% was independently linked to a reduced FEV1, VC, $FEF_{25/75}$ and SpO_2 and to an increased RV, RV:TLC, Rrs(0) and Rrs(1) (table 3). The extent of a reticular pattern was associated with a reduced Rrs(0) and Rrs(1) (table 3).

Table 2 Results of multivariate analysis with the segmental A/B ratio as a predictor

Lung function	HRCT	R^2	B (95% CI)	p Value
FEV_1	Segmental A/B ratio	0.40	−0.636 (−0.937 to −0.335)	<0.0001
VC	Segmental A/B ratio	0.42	−0.561 (−0.855 to −0.267)	0.0002
	Bands		−0.288 (−0.563 to −0.013)	0.0397
$FEF_{25/75}$	Segmental A/B ratio	0.19	−0.447 (−0.772 to −0.122)	0.0070
TLC	Bands	0.11	−0.336 (−0.670 to −0.001)	0.0484
RV	Segmental A/B ratio	0.32	0.478 (0.168 to 0.788)	0.0026
	GGO score		−0.344 (−0.645 to −0.043)	0.0249
RV:TLC	Segmental A/B ratio	0.40	0.623 (0.312 to 0.934)	0.0001
Rrs(0)	Segmental A/B ratio	0.32	0.431 (0.104 to 0.758)	0.0098
	Reticular pattern		−0.497 (−0.827 to −0.167)	0.0032
Rrs(1)	Segmental A/B ratio	0.33	0.554 (0.232 to 0.876)	0.0008
	Reticular pattern		−0.316 (−0.620 to −0.012)	0.0414
SpO_2	Segmental A/B ratio	0.22	−0.466 (−0.789 to −0.143)	0.0047

HRCT, high-resolution CT; GGO, ground glass opacification; RV:TLC, residual volume:total lung capacity ratio; VC, vital capacity.

Table 3 Results of the multivariate analysis with CSA <5 mm% as a predictor

Lung function	HRCT	R^2	B (95% CI)	p Value
FEV_1	CSA<5 mm%	0.52	−0.666 (−0.948 to −0.384)	<0.0001
	Curvilinear bands		−0.213 (−0.458 to 0.032)	0.0885
VC	CSA<5 mm%	0.51	−0.721 (−1.006 to −0.436)	<0.0001
				0.0209
$FEF_{25/75}$	CSA<5 mm%	0.26	−0.508 (−0.826 to −0.190)	0.0018
TLC	Bands	0.11	−0.336 (−0.670 to −0.002)	0.0484
RV	CSA<5 mm%	0.36	0.518 (0.213 to 0.823)	0.0009
RV:TLC	CSA<5 mm%	0.61	0.763 (0.468 to 1.058)	<0.0001
Rrs(0)	CSA<5 mm%	0.34	0.422 (0.122 to 0.722)	0.0058
	Reticular pattern		−0.516 (−0.836 to −0.196)	0.0016
Rrs(1)	CSA<5 mm%	0.58	0.748 (0.458 to 1.038)	<0.0001
	Reticular pattern		−0.516 (−0.964 to −0.068)	0.0237
SpO_2	CSA<5 mm%	0.36	−0.593 (−0.913 to −0.273)	0.0003

HRCT, high-resolution CT; RV:TLC, residual volume:total lung capacity ratio; VC, vital capacity.

Table 4 Pulmonary function results at initial and follow-up assessment

	2003–2005	2009–2010	p Value
FEV_1	80.6 (41.9–115.4)	70.9 (25.5–98.4)	0.0004
VC	80.5 (48.4–102.3)	74.5 (27.1–106.6)	0.0347
FEV_1:VC	104.8 (90.9–129.3)	98.7 (74.0–113.0)	0.0261
$FEF_{25/75}$	87.0 (33.5–136.3)	70.1 (19.6–129.2)	0.0033
TLC	87.6 (67.2–107.0)	85.5 (63.8–109.6)	0.5628
RV	87.6 (46.3–125.0)	90.0 (50.1–162.6)	0.1213
RV:TLC	102.0 (56.1–160.4)	111.1 (64.6–197.0)	0.0383
DLCOc	74.1 (42.7–104.1)	74.3 (45.3–104.8)	0.9879
KCOc	111.5 (85.0–154.9)	104.8 (77.0–137.8)	0.0325
SpO_2(%)*	97 (84–99)	97 (85–100)	0.4380

*Data are expressed as median (range) and presented as per cent predicted for height, age and sex unless indicated.
RV:TLC, residual volume:total lung capacity ratio; VC, vital capacity.

Echocardiography results

The median TRV was 2.65 (range 1.19–3.60) (m/s), the median estimated PAP 33.5 (range 9.0–70.0) (mm Hg), the median CO 6.0 (range 3.3–9.1) (L/min) and the median RVDV 93.9 (range 36.7–182.6) (mL). The median TAPSE was 2.30 (1.00–3.95) (cm), and the median E/e′ ratio was 7.60 (4.70–16.60). Significant correlations were observed between CO and the A/B ratio (r=0.41, p=0.0120) and the CSA<5 mm% (r=0.35, p=0.0440), but not with the estimated PAP. There was a correlation of CSA<5 mm% with E/e′ (r=0.45, p=0.009). There was also a correlation of CSA<5 mm% with TAPSE (r=−0.38, p=0.035), but only one subject had an abnormal TAPSE result (<1.5) and thus we cannot comment on the relationship between HRCT indices of vascular dilatation and echo indices of RV dysfunction.

The segmental A/B ratio and the CSA<5 mm% were significantly correlated with the haemoglobin level (r=−0.50, p=0.0021; r=−0.42, p=0.0090, respectively) and the lactate dehydrogenase (LDH) level (r=0.33, p=0.0450; r=0.33, p=0.0492, respectively). The segmental A/B ratio was related to the bilirubin level (r=0.47, p=0.0037) and the CSA<5 mm% to the reticulocyte count (r=0.39, p=0.0167).

Longitudinal analysis

The lung function results of the 20 patients who were reassessed had declined significantly (table 4). There were, however, no significant changes seen in the prevalence or extent/severity of lung parenchymal abnormalities on CT, but both the median segmental A/B ratio and CSA<5 mm% had increased significantly over the follow-up period (table 5). The percentage change from baseline in the A/B ratio correlated negatively with that in FEV_1 (r=0.330, p=0.0156) and carbon monoxide transfer coefficient, corrected for haemoglobin concentration (KCO) (r=−0.554, p=0.0139) and positively with that in RV (r=0.475, p=0.0342) and RV:TLC (r=−0.557, p=0.0107). The percentage change from baseline in CSA<5 mm% correlated negatively with that in FEV_1 (r=−0.330, p=0.0079) and VC (r=−0.487, p=0.0357) and positively with RV:TLC (r=0.557, p=0.0164). Logistic regression demonstrated that a higher CSA<5 mm% at baseline was predictive of a subsequent overall deterioration in HRCT appearance, that is, a gestalt change score of 1 (OR 2.62 (95% CI 1.14 to 6.01) per unit increase in CSA<5 mm%,

p=0.023). Linear mixed model analysis demonstrated a significant association of baseline CSA<5 mm% with subsequent decline in TLC, with an increased decline of −1.84 (95% CI −3.31 to −0.37) per year for each unit increase in CSA<5 mm% at baseline, p=0.014. CSA<5 mm% was also predictive of a more rapid change in RV:TLC, with a change in slope of +4.93 (95% CI 0.88 to 8.99) per year per unit increase in CSA<5 mm% at baseline, p=0.017.

DISCUSSION

We have demonstrated that pulmonary vascular abnormalities on HRCT were significantly related to pulmonary function impairment in adults with SCD. The segmental A/B ratio and CSA<5 mm% were independently linked to reductions in FEV_1, VC and $FEF_{25/75}$ and to increased respiratory system resistance and RV:TLC. In addition, small vessel size correlated with reduced oxygen saturation and haemoglobin concentration and increased LDH, bilirubin and reticulocyte levels. Those results suggest relationships between anaemia, haemolysis, hypoxia and pulmonary function abnormalities. We found a positive correlation between CSA<5 mm% (a measure of distal arteries and veins) and E/e′ which is a marker of left atrial filling pressure that is elevated if there is LV diastolic dysfunction. A higher E/e′ would result in some elevation of pulmonary venous pressure, and this result suggests a role for precapillary and postcapillary pulmonary vascular changes in SCD-related lung

Table 5 High-resolution CT (HRCT) parenchymal and vascular analysis at initial[7] and follow-up assessment

HRCT pattern	Initial Extent/severity	Follow-up Extent/severity	p Value
Reticular pattern	5.4 (0.0–17.5)	5.8 (0–17.5)	0.1987
Ground glass opacification score	0 (0–3)	0 (0–3)	0.3458
Decreased attenuation	1.3 (0.0–16.7)	1.3 (0.0–16.7)	0.9793
Consolidation	0.0 (0.0–4.2)	0.0 (0.0–1.7)	0.5000
Lobar volume loss	1 (0–7)	1 (0–7)	1.0000
Linear bands	1 (0–5)	1.5 (0–6)	0.0961
Subpleural curvilinear lines	0 (0–2)	0 (0–2)	0.0890
A/B ratio	1.26 (0.90–1.70)	1.50 (1.05–2.50)	0.0347
CSA<5 mm%	0.26 (0.14–0.52)	0.54 (0.22–1.10)	<0.0001

Data are presented as median (range).

disease. There was a negative relationship with vascular dimensions and VC, FEV_1, $FEF_{25/75}$ and SpO_2 and a positive relationship with RV, RV:TLC, Rrs(0) and Rrs(1), suggesting vascular dimensions were related to an obstructive defect. VC, FEV and $FEF_{25/75}$, however, can be reduced in both obstruction and restriction and thus the correlations with markers of vascular dilation and reductions in VC, FEV1 and $FEF_{25/75}$ may also indicate a relationship between vascular dilation and the development of restrictive lung function.

In our cohort, 23% of patients had evidence of a restrictive lung function defect and 17% had evidence of an obstructive defect. Those results are consistent with those of Santoli et al[5] but differ from those of Klings et al,[3] who found a much lower incidence of airflow obstruction. The differences may be due to a number of factors. We used a recently reported ethnic-specific reference range for spirometry,[21] whereas Klings et al[3] used a Caucasian reference range with fixed correction factors to adjust for ethnicity. We classified abnormalities based on the lower limit of normal based on percentiles recommended by the American and European Thoracic Societies,[22] whereas Klings et al used a fixed percentage predicted value to define the lower limit of normal for all lung function indices, which does not take into account that the limits of the normal range vary with age, sex and ethnicity. Furthermore, the classification scheme in the Kling's study specified that in order to be classified as obstructive or mixed, the DLCO had to be normal, which precluded the possibility that impaired gas transfer coexisted with airway abnormalities.

Restrictive lung function defects, that is, a reduced TLC and RV, were not associated with the extent of ground glass opacification or a reticular pattern and showed only a modest association with linear bands, suggesting interstitial fibrosis may not be the predominant mechanism for loss of lung volume in patients with SCD. Indeed, most CT markers of pulmonary fibrosis showed no association with reductions in VC, FEV_1, $FEF_{25/75}$, RV:TLC SpO_2, Rrs(0) or Rrs(1). The extent of a reticular pattern was associated with a reduction in respiratory system resistance; we speculate that this might be due to the tractional effects of areas of fibrosis on adjacent bronchi. Subpleural curvilinear bands were noted in 26% of patients; this is an unusual CT sign, formerly believed to be pathognomonic of early asbestosis.[23] Subpleural curvilinear bands have subsequently been described in association with micro-atelectasis in patients with atrial septal defect[24] or respiratory muscle weakness[25] and as reversible sign caused by interstitial oedema resulting from pulmonary congestion.[26] Observations in subjects without lung disease and undergoing lymphography have led to the suggestion that the sign may represent an engorged subpleural lymphatic network.[27] Given the presence of a high-output state in SCD, and the correlation of subpleural curvilinear lines with markers of small-vessel dilation observed in our cohort, it is tempting to speculate that this pattern may be related to interstitial oedema and/or increased lymphatic drainage.

We highlight a decline in lung function over a mean of 6.6 years in adults with SCD. A significant decrease was observed in VC, FEV1, $FEF_{25/75}$, FEV1:VC and KCOc with a significant increase in RV:TLC. There were no significant changes in the results of the CT assessments other than in vascular dimension assessments, where both the A/B ratio and CSA<5 mm% significantly increased. Those results suggest changes in pulmonary vascular dimensions may be responsible for the decline in lung function. Furthermore, a greater baseline CSA<5 mm% was predictive of a more rapid progression of both obstructive (increasing RV:TLC) and restrictive (decreasing

TLC) lung disease and an increased likelihood of a deterioration in parenchymal disease, as evidenced on HRCT examination. Our results emphasise the phenotypic heterogeneity of SCD lung disease. The changes in vascular morphology related to obstructive defects and the likelihood of deteriorating interstitial lung disease, suggesting that there may be a shared mechanism involving small pulmonary vessels. Field et al[28] demonstrated that bone marrow-derived fibrocytes may be mobilised into the circulation and subsequently extravasate into the lungs of SCD mice. There they function as mesenchymal progenitor cells for the production of extracellular matrix and contribute to the development of fibrosis. Elevated levels of circulating fibrocytes have been observed in humans with SCD.[28] We, therefore, speculate that pulmonary vascular engorgement and distension may potentiate extravasation of circulating fibrocytes.

This study has strengths, but some limitations too. A strength of this study was the use of two different quantitative methods for assessing pulmonary vascular morphology, the segmental A/B ratio and CSA<5 mm%, which yielded similar results. We used ethnic-specific references for spirometric indices, but the static lung volume results were related to reference ranges derived from Caucasian subjects with a fixed correction factor to account for ethnicity. All the study population were African or Caribbean, thus correlations within the cohort and comparisons between results at baseline and follow-up were valid. A limitation is that we did not have right heart catheterisation data for pulmonary artery pressures and resistance, but all the patients underwent the same echocardiographic protocol. Studies have demonstrated a minority of patients with elevated TRV have elevated pulmonary artery pressure. In a recent study, only 8 of 26 patients with elevated TRV at echocardiography had elevated pulmonary artery pressure confirmed by right heart catheterisation[29] and similar findings were reported in a larger study with 10.4% of 243 patients with elevated TRV having pulmonary hypertension.[30] It should be noted, however, that a TRV of >2.5 m/s (corresponding to an estimated mPAP greater than or equal to approximately 2 SDs above normal) does not meet the criteria for right-heart catheter-defined pulmonary arterial hypertension (mPAP >25 mm Hg), which is 3 SDs above normal. The latter corresponds to a TRV of approximately 3.0 m/s, which occurs in only about one-third of patients. Different HRCT protocols were used in our earlier study,[7] and in this study, however, care was taken to ensure that all the images used for comparisons were from anatomically comparable sections. In addition, scoring was undertaken by observers who were blinded to the results of lung function and echocardiography results. The consistent relationship between CSA<5 mm%, A/B ratio and lung function test results suggests the different protocols did not adversely influence our results. We have shown that, if TLV_{CT} is measured, volumetric HRCT scans are able to capture both restrictive and obstructive functional abnormalities, providing an alternative method to assess global pulmonary impairment in patients with SCD.

In conclusion, we have demonstrated an association between small-vessel pulmonary vascular dimensions on HRCT reflecting pulmonary vascular volume, lung function abnormalities and echocardiographic estimates of CO and ventricular function in adults with SCD. Our results suggest that abnormalities in pulmonary vascular volumes may explain some of the lung function abnormalities and the decline in lung function seen in adults with SCD.

REFERENCES

1 Piel FB, Patil AP, Howes RE, et al. Global epidemiology of sickle haemoglobin in neonates: a contemporary geostatistical model-based map and population estimates. *Lancet* 2013;381:142–51.
2 Powars D, Weidman JA, Odom-Maryon T, et al. Sickle cell chronic lung disease: prior morbidity and the risk of pulmonary failure. *Medicine (Baltimore)* 1988;67:66–76.
3 Klings ES, Wyszynski DF, Nolan VG, et al. Abnormal pulmonary function in adults with sickle cell anemia. *Am J Respir Crit Care Med* 2006;173:1264–69.
4 Delclaux C, Zerah-Lancner F, Bachir D, et al. Factors associated with dyspnea in adult patients with sickle cell disease. *Chest* 2005;128:3336–44.
5 Santoli F, Zerah F, Vasile N, et al. Pulmonary function in sickle cell disease with or without acute chest syndrome. *Eur Respir J* 1998;12:1124–29.
6 Girgis RE, Qureshi MA, Abrams J, et al. Decreased exhaled nitric oxide in sickle cell disease: relationship with chronic lung involvement. *Am J Hematol* 2003;72:177–84.
7 Sylvester KP, Desai SR, Wells AU, et al. Computed tomography and pulmonary function abnormalities in sickle cell disease. *Eur Respir J* 2006;28:832–38.
8 Ataga KI, Moore CG, Jones S, et al. Pulmonary hypertension in patients with sickle cell disease: a longitudinal study. *Br J Haematol* 2006;134:109–15.
9 Gladwin MT, Sachdev V, Jison ML, et al. Pulmonary hypertension as a risk factor for death in patients with sickle cell disease. *N Engl J Med* 2004;350:886–95.
10 Miller AC, Gladwin MT. Pulmonary complications of sickle cell disease. *Am J Respir Crit Care Med* 2012;185:1154–65.
11 Vichinsky EP. Pulmonary hypertension in sickle cell disease. *N Engl J Med* 2004;350:857–59.
12 Parent F, Bachir D, Inamo J, et al. A hemodynamic study of pulmonary hypertension in sickle cell disease. *N Engl J Med* 2011;365:44–53.
13 De Castro LM, Jonassaint JC, Graham FL, et al. Pulmonary hypertension associated with sickle cell disease: clinical and laboratory endpoints and disease outcomes. *Am J Hematol* 2008;83:19–25.
14 Chaudry RA, Cikes M, Karu T, et al. Paediatric sickle cell disease: pulmonary hypertension but normal vascular resistance. *Arch Dis Child* 2011;96:131–36.
15 Haque AK, Gokhale S, Rampy BA, et al. Pulmonary hypertension in sickle cell hemoglobinopathy: a clinicopathologic study of 20 cases. *Hum Pathol* 2002;33:1037–43.
16 Wedderburn CJ, Rees D, Height S, et al. Airways obstruction and pulmonary capillary blood volume in children with sickle cell disease. *Pediatr Pulmonol* Published Online First: 8 Jul 2013. doi: 10.1002/ppul.22845
17 Coche E, Pawlak S, Dechambre S, et al. Peripheral pulmonary arteries: identification at multi-slice spiral CT with 3D reconstruction. *Eur Radiol* 2003;13:815–22.
18 Matsuoka S, Washko GR, Yamashiro T, et al. Pulmonary hypertension and computed tomography measurement of small pulmonary vessels in severe emphysema. *Am J Respir Crit Care Med* 2010;181:218–25.
19 Matsuoka S, Washko GR, Dransfield MT, et al. Quantitative CT measurement of cross-sectional area of small pulmonary vessel in COPD: correlations with emphysema and airflow limitation. *Acad Radiol* 2010;17:93–9.
20 Rudski LG, Lai WW, Afilalo J, et al. Guidelines for the echocardiographic assessment of the right heart in adults: a report from the American Society of Echocardiography endorsed by the European Association of Echocardiography, a registered branch of the European Society of Cardiology, and the Canadian Society of Echocardiography. *J Am Soc Echocardiogr* 2010;23:685–13; quiz 786–88.
21 Quanjer PH, Stanojevic S, Cole TJ, et al.: ERS Global Lung Function Initiative. Multi-ethnic reference values for spirometry for the 3–95 year age range: the global lung function 2012 equations. *Eur Respir J* 2012;40:1324–43.
22 Pellegrino R, Viegi G, Brusasco V, et al. Interpretative strategies for lung function tests. *Eur Respir J* 2005;26:948–68.
23 Akira M, Yamamoto S, Yokoyama K, et al. Asbestosis: high-resolution CT-pathologic correlation. *Radiology* 1990;176:389–94.
24 Yamaki S, Abe A, Sato K, et al. Microatelectasis in patients with secundum atrial septal defect and its relation to pulmonary hypertension. *Jpn Circ J* 1997;61:384–89.
25 Estenne M, Gevenois PA, Kinnear W, et al. Lung volume restriction in patients with chronic respiratory muscle weakness: the role of microatelectasis. *Thorax* 1993;48:698–701.
26 Arai K, Takashima T, Matsui O, et al. Transient subpleural curvilinear shadow caused by pulmonary congestion. *J Comput Assist Tomogr* 1990;14:87–8.
27 Pilate I, Marcelis S, Timmerman H, et al. Pulmonary asbestosis: CT study of subpleural curvilinear shadow. *Radiology* 1987;164:584.
28 Field JJ, Burdick MD, DeBaun MR, et al. The role of fibrocytes in sickle cell lung disease. *PLoS One* 2012;7:e33702.
29 Fonseca GH, Souza R, Salemi VM, et al. Pulmonary hypertension diagnosed by right heart catheterisation in sickle cell disease. *Eur Respir J* 2012;39:112–18.
30 Mehari A, Gladwin MT, Tian X, et al. Mortality in adults with sickle cell disease and pulmonary hypertension. *JAMA* 2012;307:1254–6.

Pulmonary function, computed tomography and echocardiographic abnormalities in sickle cell disease

On line data supplement

Lung function assessments

Patients were assessed in the Amanda Smith Pulmonary Function Laboratory at King's College Hospital NHS Foundation Trust. No subject underwent lung function testing within two weeks of an upper respiratory tract infection or within a month of suffering a vaso-occlusive crisis. A history was taken of past and current respiratory symptoms and medication for respiratory problems. Standing height was measured using a wall-mounted stadiometer (Holtain ltd, Crymych, Dyfed, UK) and weight using electronic weighing scales (Seca ltd, Birmingham, UK).

Measurements were performed using a pneumotachograph based system (Jaeger Masterscreen PFT, Carefusion Ltd, Basingstoke UK). Results were expressed as percent predicted for height, age, and sex using the ethnic-specific reference equations for spirometry-[E1] and the European Community for Steel and Coal Statement of the European Respiratory Society reference equations for lung volumes and gas transfer.[E2] Spirometry, static lung volumes using whole-body plethysmography and transfer factor for carbon monoxide were assessed according to American Thoracic Society/European Thoracic Society guidelines.[E3-E5] The mean respiratory system resistance (Rrs(0)) and frequency dependence of resistance (Rrs(1)) from 5-25Hz were measured using impulse oscillometry and expressed as the percent predicted for height, weight, and age.[E6] The frequency dependence of resistance was assessed using the mean slope of the resistance-frequency

curve over the range 5 to 25Hz. Respiratory resistance was considered to be elevated if Rrs(0) was greater than the upper limit of normal. Spirometry was repeated following administration of a bronchodilator (400µg salbutamol via a MDI and spacer) and a positive response was defined as an increase in FEV_1 of greater than or equal to 12% from baseline and an increase of at least 200ml. Oxygen saturation was measured using a pulse oximetry (Masimo Radical 7 and a rainbow probe, Masimo, California, USA).

The predicted values for total lung capacity were reduced by 12%, and residual volume by 7% to correct for ethnicity.[E7] The lower and upper limits of normal were defined as the fifth and ninety-fifth percentiles respectively of the appropriate reference range. Patients were diagnosed as having a restrictive abnormality if their TLC was less than the lower limit of normal (LLN), with a normal FEV1:VC. An obstructive abnormality was diagnosed if the FEV1:VC was less than the LLN with a normal VC, or if VC was less than the LLN with a normal TLC and an RV:TLC greater than the upper limit of normal (ULN). A mixed abnormality was diagnosed if the TLC and FEV1:VC were less than the LLNs .

Computed tomography

Patients were scanned on a 64-channel multidetector CT machine (GE 64 VCT Lightspeed machine; GE Healthcare, Waukesha, Wisconsin, USA; 100 kV, Auto mA/Smart mA; pitch

1.375, 0.5 sec tube rotation, beam collimation 40 mm, detector size 0.65 mm). Contrast was injected at a rate of 4-5 ml/s and scanning was performed cranio-caudally with the subject in a supine position and breathing suspended at maximal inspiration. The period of CT scanning was timed to coincide with optimal contrast opacification of the pulmonary arterial tree using bolus-tracking. In the earlier study-[E8] patients had been imaged using a dual-detector CT machine (HiSpeed NX/I; GE Medical Systems, Waukesha, Milwaukee, Wisconsin, USA). Interspaced HRCT images (1.5mm collimation at 10 mm intervals) had been acquired at total lung capacity, in the supine and prone positions. Images were reconstructed using a high-spatial-frequency (bone) algorithm. All CT studies were securely stored on CD for subsequent review.

CT patterns-[E9] were quantified i) to the nearest 5%; ii) on a semiquantitative scale or iii) for their presence or absence, as appropriate. The following CT patterns were quantified to the nearest 5%: i) reticular pattern defined as innumerable interlacing line shadows which, by summation, produce an appearance resembling a mesh; ii) ground-glass opacification (defined as a hazy increased lung opacity in which the visibility of bronchial and vascular margins were preserved); iii) areas of decreased attenuation as part of a mosaic attenuation pattern defined as a patchwork of areas of differing lung densities and iv) consolidation defined as a homogeneous increase in lung parenchymal attenuation which obscures the margins of airway and vessel walls. In patients with consolidation, the extent to the nearest 5% of sub-pleural consolidation was also recorded. For ground glass opacification, a score was assigned based on the observed extent (0=none; 1= <10% extent; 2= 10-50% extent; 3 >50% extent). The following CT signs were scored semi-quantitatively: i) thickening of interlobular septa (0=none; 1= <5 thickened interlobular septa [ILS]; 2= >5 thickened ILS or

<50% pleural surface involved; 3= >50% pleural surface involved or 4 = diffusely thickened

ILS), ii) lobar volume loss (0=none; 1=mild or 2=severe). The presence or absence of the

following signs were recorded: i) traction bronchiectasis defined as irregular

bronchial/bronchiolar dilatation caused by surrounding retractile pulmonary fibrosis in a

reticular pattern and/or ground-glass opacification; ii) linear bands of attenuation; iii) sub-

pleural curvilinear lines defined as a thin curvilinear opacity of 1-3 mm thickness and lying

within one centimetre of and parallel to the pleural surface and iv) pulmonary infarcts defined

as a peripheral irregular opacity associated with a linear opacity no more than 2 cm in length.

Whole-lung scores were produced by taking the mean of all lobes for signs which had been

measured to the nearest 5% and by summing the lobar scores for signs recorded as

present/absent. Vascular dimensions were assessed in two ways. First, proprietary electronic

callipers were used to measure the widest short axis diameters of the upper lobe apical or

apico-posterior segmental arteries and the lower lobe posterobasal segmental arteries together

with the widest external short axis diameter of the corresponding segmental bronchi on the

same axial image in at least three out of four lobes.[E10] Based on those measurements, the

mean segmental artery/ bronchus (A/B) ratio in at least three out of four lobes was calculated.

Distal vessel dimensions, including both arteries and veins at the subsubsegmental level-

[E11] were measured using the method of Matsuoka *et al.*[E12, E13] Three CT slices were

selected from each examination. The upper cranial slice was located approximately one

centimetre above the upper margin of the aortic arch, the middle slice approximately one

centimetre below the carina, and the lower caudal slice approximately one centimetre below

the right inferior pulmonary vein. The measurements were performed using the Java-based

semi-automated image analysis software 'ImageJ' (Rasband, W.S., ImageJ, U. S. National

Institutes of Health, Bethesda, Maryland, USA, http://imagej.nih.gov/ij/, 1997-2012). Before processing, each selected image was smoothed using Gaussian blurring to filter image noise. The lung field was then segmented using a thresholding technique to include all pixels between -500 and -1024 Hounsfield Units (HU) (Figure 1) and the segmented image was converted to a binary image with a window level of -760 HU (Figure 1). The 'Analyze Particles' function was then used to count and measure the cross-sectional area of vessels within a range of 0-5mm^2. The 'Circularity' function was then used to select only those vessels running approximately perpendicular to the scan plane based on their apparent shape in the slice image, setting the circularity range to 0.9-1.0. The total summated cross-sectional area for those vessels was then expressed as a percentage of the total lung area of the three selected slices using threshold values between -500 HU and -1024 HU (CSA<5mm%).

The segmental A/B ratio has been shown to correlate with pulmonary artery pressure in a mixed cohort of patients with lung disease [E14]. CSA<5mm% has been measured in patients with HRCT-defined emphysema due to COPD and has been shown to correlate with pulmonary artery pressure in this group.[E12, E13]

CT total lung volume (TLV$_{CT}$), comprising air plus tissue components, was derived using a proprietary lung segmentation algorithm (Apollo, Vida Core Lab Services, Vida Diagnostics Inc, Iowa, USA) which uses a localized and adaptive threshold method to delineate lung tissue on a lobar basis from surrounding tissues (Figure 2). The TLV$_{CT}$ was not available for the scans obtained in 2003-2005.

For the longitudinal analyses, initial and follow-up CT scans were compared. Two observers identified anatomically comparable sections as judged by vascular and bronchial landmarks on the two CT scans from each individual and recorded their impression of whether the overall appearance of the interstitium on the follow-up scan compared to the initial scan had

deteriorated. Patients who had deteriorated were assigned a 'gestalt' change score of 'one' and those who did not were scored as zero.

Statistical analysis

Data were tested for normality using the D'Agostino and Pearson omnibus normality test. Comparisons, as appropriate, were made with t-tests or Mann-Whitney U tests and paired analyses were performed using paired-sample t-tests or Wilcoxon matched-pairs signed rank tests. In the longitudinal cohort, we used non-parametric tests for baseline-follow up comparisons as we felt that the number of patients was too small too meaningfully perform normality testing. For the descriptive data in the larger cohort (n=35), who were tested once, data were displayed as median (range) to demonstrate the wide range in lung function. On HRCT, whilst GGO score, bands, curvilinear bands, and A/B ratio were not normally distributed, the residuals in all of the final regression models did not differ significantly from a normal distribution (Pearson omnibus normality test p>0.05). The strength of relationships were assessed using the Pearson or Spearman rank correlation.   Stepwise linear regression with backward elimination was used to identify HRCT parenchymal and vascular results which correlated with the results of the lung function tests. HRCT variables examined in the preceding bivariate analyses were entered as initial predictors, unless predictors were multi-collinear. All regression models were built in the sample size n=35. All final models satisfied the assumptions of multiple linear regression as determined by assessment of homoscedasticity, no multicollinearity between predictors and normal distribution of errors.In the longitudinal cohort, exploratory models were generated to test whether baseline vascular markers predicted subsequent deterioration of parenchymal disease and progression of lung function abnormalities. Logistic regression was used to assess the effect of baseline

6

segmental A/B ratio and CSA<5mm on the deterioration in the overall CT appearance ('Gestalt' change score) and linear mixed model analysis (LMM) to predict individual decline in lung function results.

Haematological data

Haemoglobin, lactate dehydrogenase (LDH), bilirubin levels and reticulocyte counts were obtained from routine blood tests taken within one month of testing when patents were clinically stable.

Thirty-five patients with a median age of 43 (range 17-73) years were assessed. Twenty of the 35 patients (median age at initial assessment 38, range 17 – 66 years) had been assessed at a median of 6.6 (range 5.5-6.7) years previously. Of the thirty-three patients who participated in the original study 20 were tested at follow-up: three had died, six were lost to follow-up three declined to participate in the follow-up study and one declined to undergo HRCT scanning and was excluded. The twenty patients who were tested at follow-up were included in the 2009-2013 cohort, together with fifteen new patients making a total of thirty-five patients.

REFERENCES

E1   Quanjer PH, Stanojevic S, Cole TJ, et al: ERS Global Lung Function Initiative. Multi-ethnic reference values for spirometry for the 3-95 year age range: the global lung function 2012 equations. *Eur Respir J* 2012;**40**:1324-43.

E2   Quanjer PH, Tammeling GJ, Cotes JE, et al. Lung volumes and forced

ventilatory flows. Report Working Party Standardization of Lung Function Tests,

European Community for Steel and Coal. Official Statement of the European

Respiratory Society. *Eur Respir J Suppl* 1993;**16**:5-40.

E3   Miller MR, Hankinson J, Brusasco V, et al. Standardisation of spirometry. *Eur

Respir J* 2005;**26**:319-38.

E4   Wanger J, Clausen JL, Coates A, et al. Standardisation of the measurement of

lung volumes. *Eur Respir J* 2005;**26:**511-22.

E5   Macintyre N, Crapo RO, Viegi G, et al. Standardisation of the single-breath

determination of carbon monoxide uptake in the lung. *Eur Respir J* 2005;**26**:720-

35.

E6   Pasker HG, Schepers R, Clement J, et al. Total respiratory impedance measured

by means of the forced oscillation technique in subjects with and without

respiratory complaints. *Eur Respir J* 1996;**9**:131-39.

E7   Pellegrino R, Viegi G, Brusasco V, et al. Interpretative strategies for lung

function tests. *Eur Respir J* 2005;**26**:948-968.

E8   Sylvester KP, Desai SR, Wells AU, et al. Computed tomography and pulmonary

function abnormalities in sickle cell disease. *Eur Respir J* 2006;**28**:832-38.

E9   Hansell DM, Bankier AA, MacMahon H, et al. Fleischner Society: glossary of

terms for thoracic imaging. *Radiology* 2008;**246**:697-722.

E10 Tan RT, Kuzo R, Goodman LR, et al. Utility of CT scan evaluation for predicting

pulmonary hypertension in patients with parenchymal lung disease. Medical

College of Wisconsin Lung Transplant Group. *Chest* 1998;**113**:1250-6.

E11 Coche E, Pawlak S, Dechambre S, et al. Peripheral pulmonary arteries: identification at multi-slice spiral CT with 3D reconstruction. *Eur Radiol* 2003;13:815-22.

E12 Matsuoka S, Washko GR, Yamashiro T, et al. Pulmonary hypertension and computed tomography measurement of small pulmonary vessels in severe emphysema. *Am J Respir Crit Care Med* 2010;**181**:218-25.

E13 Matsuoka S, Washko GR, Dransfield MT, et al Quantitative CT measurement of cross-sectional area of small pulmonary vessel in COPD: correlations with emphysema and airflow limitation. *Acad Radiol* 2010;**17**:93-9.

E14 Devaraj A, Wells AU, Meister MG, et al. Detection of pulmonary hypertension with multidetector CT and echocardiography alone and in combination. *Radiology* 2010;**254**:609-16.